Chemical Engineering Journal 162 (2010) 591–598

Contents lists available at ScienceDirect

Chemical Engineering Journal

journal homepage: www.elsevier.com/locate/cej

Untreated clay with high adsorption capacity for effective removal of C.I. Acid Red 88 from aqueous solutions: Batch and dynamic flow mode studies

Sibel Tunali Akar*, Recep Uysal

Department of Chemistry, Faculty of Arts and Science, Eskişehir Osmangazi University, Turkey

ARTICLE INFO

Article history:
Received 16 April 2010
Received in revised form 30 May 2010
Accepted 2 June 2010

Keywords:
Dye
Clay
Adsorption
Kinetics
Isotherm

ABSTRACT

Batch and dynamic flow adsorption studies were carried out using natural clay for the removal of Acid Red 88 (AR88) dye from aqueous solutions. Adsorption conditions were examined with respect to initial pH, adsorbent amount, contact time, initial dye concentration, column i.d. and flow rate. Adsorption process was better described by the pseudo-second-order kinetic and Langmuir isotherm models. SEM and zeta potential analysis were used to characterize the adsorbent material. 98.10 ± 0.34% of dye could be removed in 15 min at pH 2.0 in the batch mode. The adsorbent exhibits very high monolayer dye binding capacity of 1133.10 mg g^{-1} which was comparable to or higher than those of many sorbent materials. Our results indicate that the suggested natural and low-cost adsorbent material may be useful for the effective removal of contaminating acid dyes.

1. Introduction

Contamination of waters, due to discharge of untreated or partially treated industrial wastewaters into the ecosystem, has become a common problem for many countries [1,2]. In particular, synthetic dyes from industrial effluents such as textile, paper, dyeing, printing, food, etc. cause serious problems to human health and environment. The number of commercially available dyes is more than 100,000 and the annual production of these exceeds one million tons worldwide [3,4]. The dyes used in the textile industries include several structural varieties such as acidic, reactive, basic, disperse, azo, diazo, anthraquinone based and metal complex dyes [1]. More than 50% of the world production of dyes consists of azo dyes [5]. They are aromatic compounds including one or more azo groups (–N=N–) and may also contain sulfonate groups [3,4]. Azo dyes cannot be easily removed by conventional treatment processes due to their stability under light, heat, oxidizing agents and biological degradation. In the degradative conditions cleavage of azo linkages in their structure can produce toxic aromatic amines. These derived compounds can exhibit more toxic effects to the environment than the parent compound [6]. Therefore, the effective treatment of dye contaminated effluents is currently a primary environmental concern.

Adsorption technology has attracted interest in this context as an effective and alternative treatment process and has many advantages over the existing conventional process. This process is not only economic and feasible but also produces high quality of water [7,8]. The dye adsorption potentials of many low-cost and natural materials have previously been reported upon, including *Thuja orientalis* [9], hazelnut shell [10], macro-fungus [11], baggase pith [12], *Pyracantha coccinea* [13], kidney bean [14], calcined alunite [15]. On the other hand some modification procedures were applied to improve the adsorption performances and characteristics of the adsorbent materials [16–18].

In the present study we reported the very high adsorption potential of natural clay for C.I. Acid Red 88 (AR88) dye. Our previous findings indicated that this cost-effective and readily available natural material could be employed as an effective adsorbent in chemically modified form for the removal of chromium (VI) ions [19]. In order to keep the cost of dye treatment low, the adsorbent clay employed in the present study was used without any pretreatment or other modification. AR88 was selected as a representative adsorbate for this study due to its wide use in dyeing textile fabrics, silk, nylon, wool and leather [3] and carcinogenic effects of degradation byproducts (such as toxic aromatic amines) [20]. Adsorptive removal of AR88 onto clay was investigated in batch and dynamic flow modes of operation. Adsorption process variables such as initial pH, adsorbent dosage, contact time, temperature, flow rate and column diameter were investigated. Equilibrium adsorption data were modeled with Langmuir, Freundlich, Dubinin–Radushkevich (D–R) isotherm models and the pseudo-first-order, the pseudo-second-order, intraparticle diffusion and Elovich kinetic models. SEM and zeta potential measurement studies were carried out for the adsorbent characterization.

* Corresponding author. Tel.: +90 222 2393750/2862; fax: +90 222 2393578.
E-mail address: stunali@ogu.edu.tr (S.T. Akar).

1385-8947/$ – see front matter © 2010 Elsevier B.V. All rights reserved.
doi:10.1016/j.cej.2010.06.001

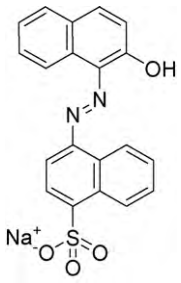

Fig. 1. Chemical structure of AR88.

2. Experimental

2.1. Adsorbent material

The clay sample used as the adsorbent in the experiments was provided from the deposits located in the region of Eskişehir-Mihalıççık, Turkey. It was prepared by grinding in a laboratory type ball-mill and sieved to size of 100 mesh fractions using ASTM standard sieves.

AR88 dye (C.I 15620, λ_{max} = 505 nm) was obtained from Sigma–Aldrich Corporation, St. Louis, MO, USA, and was used as received. The chemical structure and UV–vis spectrum of the dye were presented in Figs. 1 and 2. A stock solution (1.0 g L^{-1}) of AR88 was prepared by dissolving accurate weight amount of dye in deionized water and the other concentrations were obtained by dilution of this stock dye solution. All other chemicals used in this investigation were of analytical grade.

2.2. Adsorption studies

The batch mode adsorption studies were studied by mixing known amounts of adsorbent with 50 mL of AR88 solution at desired concentration and stirring on a digitally controlled multipoint magnetic stirrer at 200 min^{-1}. The effect of initial pH and adsorbent amount on the adsorption of acid dye onto clay was investigated within the ranges of 2.0–10.0 and 0.04–4.0 g L^{-1}, respectively. The pH of the dye solutions was adjusted to required values using negligible amount of dilute HCl or NaOH solution. In order to determine the equilibrium time, the contact time was varied between 5 and 60 min. The dye adsorption kinetics was evaluated at different temperatures of 25, 35 and 45 °C. The adsorbent was separated from the solution by centrifugation at 4500 min^{-1} for 5 min. The effect of ionic strength was investigated in the solutions including NaCl with the concentrations between 0.02 and 0.15 mol L^{-1}. Adsorption trials in dynamic flow mode were performed in small scale cylindrical packed bed columns at 25 °C. A known quantity of natural adsorbent was placed between glass wool filters in the column. Dye solution at an initial concentration of 150 mg L^{-1} and pH of 2.0 was pumped upwards through the column using a peristaltic pump (Ismatec ecoline). Tygon tubing was used for the connections. Continuous system variables studied are: adsorbent amount (0.04–0.4 g), flow rate (0.5–8.0 mL min^{-1}) and column i.d. (internal diameter) (9–19 mm).

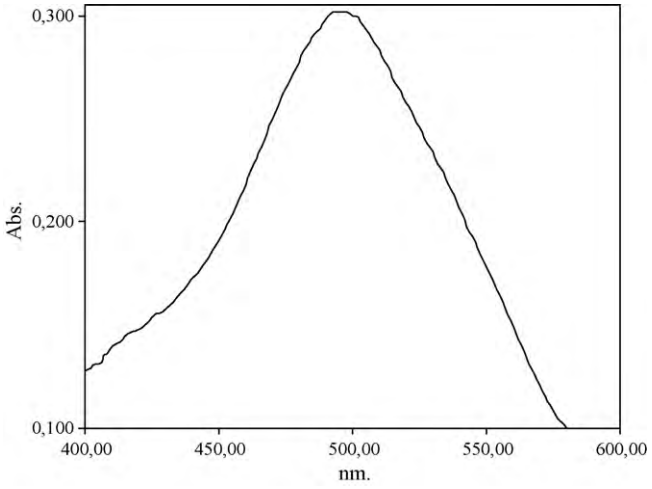

Fig. 2. UV–vis absorption spectrum of AR88 dye.

2.3. Instrumentation

The zeta potential values of the adsorbent material were measured by zeta potential analyzer (Malvern zeta sizer) in the solutions with the pH range of 2.0–10.0. After dye adsorption in batch and column systems, residual dye contents in the treated solutions were quantified by UV visible spectrometry (Shimadzu UV-2550) at maximum wavelength of dye.

The equilibrium adsorption capacity (q_e) of natural clay was calculated from the initial (C_i) and final (C_e) concentration of dye in the solutions using the following general mass-balance equation.

$$q_e = \frac{V(C_i - C_e)}{m} \quad (1)$$

where V is the solution volume (L) and m is the amount of adsorbent (g).

2.4. Statistical analysis

In order to ensure the reproducibility of results, experiments were replicated three times and data presented were the mean values from these independent experiments. Experimental errors were estimated and depicted with error bars and standard deviations are indicated wherever necessary. All statistical analysis was performed using SPSS 10.0 for Windows.

3. Results and discussion

3.1. Adsorbent characterization

On the basis of powder X-ray diffraction (XRD) profile the natural clay contained montmorillonite as a major constituent in the mineral structure. The minor components detected by XRD are analcime and feldspar (sodium aluminium silicate) [19].

SEM is one of the useful tools to characterize the surface structure of the adsorbent materials. Typical SEM micrographs of adsorbent material were taken before and after dye adsorption and presented in Fig. 3. These micrographs indicated clearly the appearance of the molecular cloud over the surface of dye-loaded clay, which was absent on the rough and porous structure of the clay before loading with dye.

In order to determine the surface charge of the adsorbent, the zeta potential values were measured as a function of pH and the results were presented in Fig. 4. As shown here, the surface charge of clay is negative and no isoelectric point (IEP) was observed in the examined pH range. Similar observations were also reported in the literature [21–24]. The net negative charge density of the adsorbent increased with increasing the pH up to 3.0 ($p < 0.05$) and stayed almost constant above this pH value ($p > 0.05$). It is well known that montmorillonite type clays carry two kinds of electrical charges namely, pH-dependent (variable) charge and structural (permanent) negative charge [25]. The permanent negative charge arises from the substitution of Al^{3+} by Mg^{2+} or Fe^{2+} and Si^{4+} by Al^{3+} in the structure of the mineral. It was reported the edges of

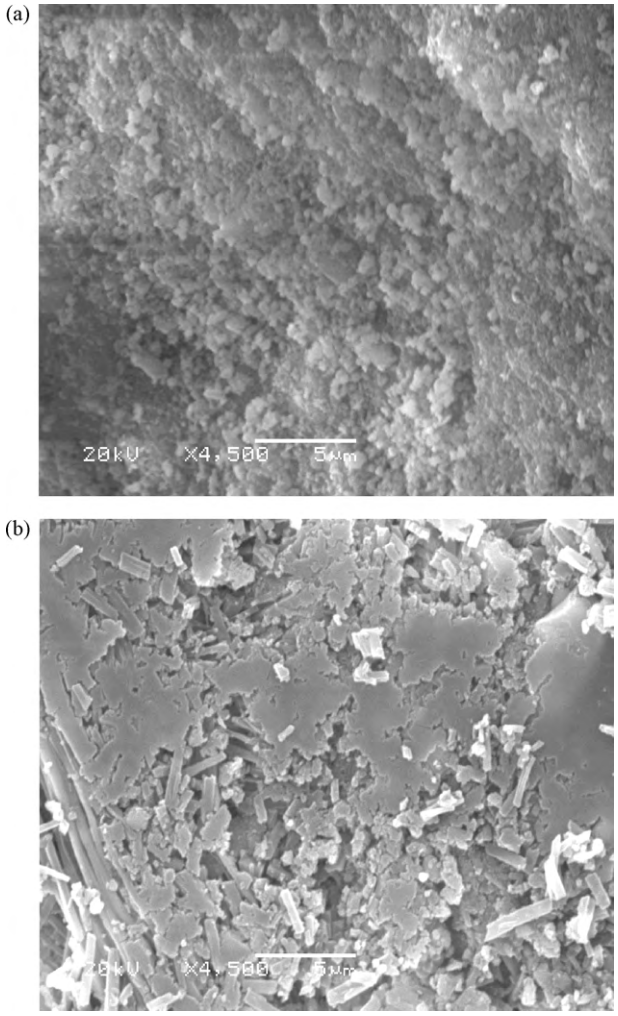

Fig. 3. SEM micrograph of untreated (a) and dye-loaded (b) clay.

montmorillonite behave as the metal oxide surface and positively charged at acidic pH values [26,27].

3.2. Effect of pH

Solution pH is one of the important parameters controlling the adsorption behavior of adsorbate onto adsorbent surface. The variation in AR88 adsorption capacity of natural clay as a function of medium pH is shown in Fig. 4. The maximum adsorption capacity was observed at pH 2.0, lessened notably with increasing the pH up to 4.0 ($p < 0.05$), remained nearly constant ($p > 0.05$) and negligible above this pH value. High adsorption capacity observed in the acidic pH values can be attributed to the electrostatic attraction forces between dye anions and positively charged parts on the clay surface. It was reported that although the overall particle charge is negative in general, at acidic conditions there were both negatively and positively charged parts on the surface of clay [28]. It could be concluded that these positively charges at the edges of clay are responsible for the adsorption of anionic dye onto clay at acidic pH values. Crini [29] reported the adsorption of dyes on clay minerals is mainly dominated by ion-exchange processes. Strongly pH-dependent adsorption trend for AR88 dye onto clay may also be explained by an ion-exchange process.

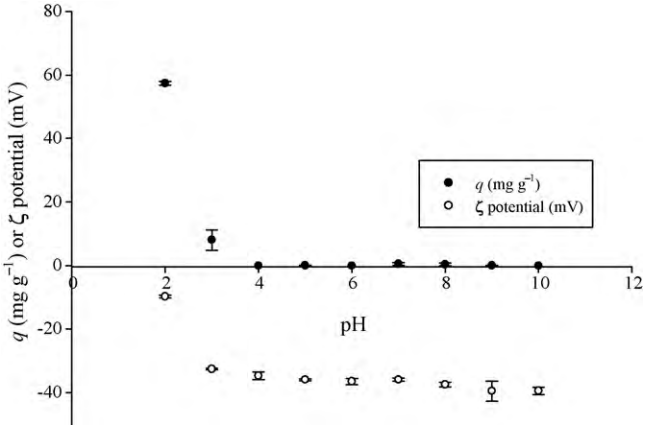

Fig. 4. Effect of pH on the adsorption of AR88 onto clay and ζ potential values of adsorbent as a function of pH.

3.3. Effect of adsorbent concentration

The dye uptake yields of natural clay for AR88 dye at various clay concentrations are examined in order to optimize the adsorbent dosage. The dye adsorption yield of natural clay increased from $93.66 \pm 1.22\%$ to $98.10 \pm 0.34\%$ when the amount of clay increased from 0.4 to 0.8 g L^{-1} ($p < 0.05$). A further increase in the adsorbent amount over 0.8 g L^{-1} did not lead to a significant change in the adsorption yield of clay due to saturation of the adsorbent surface with dye molecules and it remained nearly constant ($p > 0.05$). The optimum adsorbent amount was selected as 0.8 g L^{-1} for further batch adsorption studies. Similar trend in dye (Reactive Red MF-3B) removal with increasing adsorbent amount has also been shown by Huang et al. using organoclay material [30]. Also Almeida et al. [31] found that the dye adsorption yield of montmorillonite clay increased from about 70% to 99% when the clay amount increased from 1.6 to 3.0 g L^{-1} and this trend has been attributed to increased surface area and possible dye binding sites of adsorbent material.

3.4. Effect of contact time and temperature

Contact time is one of the important parameters for the successful application of adsorption procedures. The adsorption capacities of clay at different temperatures (25, 35 and 45 °C) as a function of time were investigated at an initial AR88 concentration of 150 mg L^{-1}. A larger amount of AR88 was removed by clay in the first 5 min of contact time. Adsorption equilibrium was established within 15 min at the end of rapid adsorption for all temperatures studied. The rate of adsorption is of great significance for developing an adsorbent material for water-treatment technology [32] and has also practical importance since it will facilitate the scale-up of the treatment process to smaller reactor volumes ensuring efficiency and economy [33]. In this study it was observed that the temperature has no significant effect on the adsorption of AR88 dye by natural adsorbent ($p > 0.05$) in the studied temperature range. Similar observations were previously reported in the literature [34].

3.5. Adsorption kinetics

The data obtained from the contact time-dependent experiments were further used to evaluate the kinetics of the adsorption process. Four kinetic models were tested to obtain rate constants, equilibrium adsorption capacity and mechanism at different temperatures, namely, pseudo-first-order [35], pseudo-second-order [36], Elovich [37] and intraparticle diffusion [38] models. The linear equations of these models are given in Appendix A and the calculated kinetic parameters in this study are represented in Table 1.

From r^2 values in Table 1, it can be clearly seen that the adsorption of AR88 onto natural clay does not follow the pseudo-

Table 1
Kinetic model constants for the adsorption of AR88 onto clay at different temperatures.

Pseudo-first-order model				Pseudo-second-order model				Intraparticle diffusion model			Elovich model		
t (°C)	k_1 (min^{-1})	q_e (mg g^{-1})	r^2	k_2 (g mg^{-1} min^{-1})	q_e (mg g^{-1})	h (mg g^{-1} min^{-1})	r^2	k_p (mg g^{-1} min$^{-1/2}$)	C (mg g^{-1})	r^2	α (mg g^{-1} min^{-1})	β (g mg^{-1})	r^2
25	2.86×10^{-2}	0.18	0.034	1.98×10^{-2}	178.67	6.32×10^{2}	0.999	1.20	169.65	0.824	5.33×10^{25}	0.349	0.904
35	2.46×10^{-2}	2.87	0.408	3.85×10^{-2}	176.67	1.20×10^{3}	0.999	0.99	169.87	0.548	1.93×10^{29}	0.389	0.685
45	2.03×10^{-2}	2.37	0.377	4.12×10^{-2}	175.42	1.27×10^{3}	0.999	0.94	168.95	0.578	8.89×10^{29}	0.410	0.748

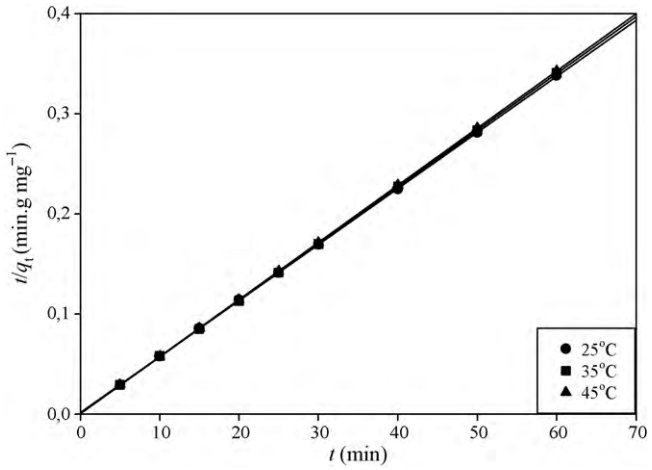

Fig. 5. Pseudo-second-order kinetic plots for the adsorption of AR88 onto clay at different temperatures.

first-order kinetic. Also the experimental q_e values did not agree with the calculated ones.

Fig. 5 shows the pseudo-second-order kinetic plots for the adsorption of AR88 onto clay at different temperatures. All correlation coefficients at different temperatures were 0.999 (Table 1) and greater than the other kinetic models studied and the calculated equilibrium adsorption capacity values showed good agreement with those obtained experimentally. The adsorption capacity values did not significantly change with increasing temperature ($p > 0.05$). However, temperature affected the kinetics of adsorption in such a way that the rate constant (overall and initial) increases with temperature. The values of k_2 were found to increase from 1.98×10^{-2} to 4.12×10^{-2} g mg^{-1} min^{-1} when the temperature increased from 25 to 45 °C. The similar effect of the temperature on the adsorption kinetics was observed by ElShafei et al. [39].

AR88 adsorption kinetics onto natural clay was also tested with the Elovich kinetic model. r^2 values in Table 1 are very low (0.904–0.748). These indicate that AR88 dye adsorption onto the natural clay cannot be described by the Elovich kinetic model.

Finally, experimental data were evaluated by the intraparticle diffusion kinetic model in order to investigate whether intraparticle diffusion is rate-limiting. According to Weber–Morris model, the plot of uptake, q_t, vs the square root of time, $t^{1/2}$, (figure not shown), should be linear if intraparticle diffusion is involved in the adsorption system and if these lines pass through the origin, then intraparticle diffusion is the rate controlling step [40]. When the plots do not pass through the origin, this is indicative of some degree of boundary layer control and this further indicates that the intraparticle diffusion is not the only rate-limiting step, but also other kinetic models may control the rate of adsorption, all of which may be operating simultaneously. Therefore the slope of linear portion of the figure is defined as rate parameter, k_p, for the intraparticle diffusion, and adsorption rate characteristic in this region where intraparticle diffusion is the rate limiting factor [41]. The correlation coefficients (r_p^2) for the intraparticle diffusion model are lower than that of the pseudo-second-order model (Table 1) but this model indicates that the adsorption of AR88 onto clay may be followed by an intraparticle diffusion model up to 40 min.

3.6. Adsorption isotherms

Adsorption isotherms indicate a distribution of adsorbate between solution and adsorbent when adsorption process reaches an equilibrium state. Giles et al. [42] proposed a general classification of adsorption isotherms. According to this classification,

Table 2
Isotherm model constants for the adsorption of AR88 onto clay.

Langmuir			Freundlich			Dubinin–Radushkevich (D–R)			
q_{max} (mol g^{-1})	K_L (L mol^{-1})	r_L^2	n	K_F (L g^{-1})	r_F^2	q_m (mol g^{-1})	β (mol^2 kJ^{-2})	r_{D-R}^2	E (kJ mol^{-1})
2.83×10^{-3}	3.02x10^4	0.998	2.079	1.56×10^{-1}	0.919	1.42×10^{-2}	3.849×10^{-3}	0.946	11.41

four main isotherm shapes, "*H*" isotherm (high affinity), "*L*" isotherm (Langmuir), "*C*" isotherm (constant partition) and "*S*" isotherm (sigmoidal-shaped) were commonly observed. In this study dye solutions at different initial concentrations in the range of 100–900 mg L^{-1} were used to investigate the Giles isotherm shape and the adsorption isotherms at different temperatures were presented in Fig. 6. As can be seen from this figure AR88/clay system in this study may be explained by *L* isotherm. Therefore, it may be concluded that the ratio between the solid and liquid concentration of adsorbate decreases when the initial adsorbate concentration increases [43,44].

Since the temperature has no significant effect on the adsorption of AR88 onto clay, experimental data at 25 °C were fitted to models of Freundlich [45], Langmuir [46] and Dubinin–Radushkevich (D–R) [47]. The adsorption constants together with the r^2 values are shown in Table 2. Isotherm equations were represented in Appendix A.

The Freundlich isotherm model is an empirical equation usually adopted for heterogeneous adsorption and frequently used to describe the adsorption processes [48,49]. Fig. 7 shows the Freundlich isotherm plot for AR88 adsorption onto clay and the values of K_F and n were 1.56×10^{-1} and 2.079, respectively.

The Langmuir isotherm plot is shown in Fig. 8. Regarding the isotherm fittings for data as may be seen in Table 2, quite high correlation coefficients ($r^2 > 0.9$) were found for all models. Nevertheless, Langmuir model seems to provide better fittings than the other models. It could be concluded from these results that the adsorption process of AR88 onto clay was monolayer and the maximum monolayer adsorption capacity was found as 2.83×10^{-3} mol g^{-1} (1133.10 mg g^{-1}). The adsorption results of AR88 reported in the literature by different sorbent materials were summarized in Table 3. The maximum adsorption capacity of clay obtained for AR88 dye in our study is comparable and was found to be moderately higher than that of many corresponding sorbent materials. Clays have larger surface area and high porosity. The higher adsorption capacity of the adsorbent used in this study may be come from these properties of clay.

R_L values indicate the type of isotherm as unfavorable ($R_L > 1$), linear ($R_L = 0$), favorable ($0 < R_L < 1$) or irreversible ($R_L < 0$) [48]. The values of R_L obtained in this study were between 1.17×10^{-1} and 1.46×10^{-2} at different initial concentrations of dye indicating that the AR88 adsorption onto clay was favorable at the conditions being studied. However Fig. 9 shows the R_L values decreased as the initial dye concentration increased. Therefore, the adsorption of AR88 was more favorable at higher concentration.

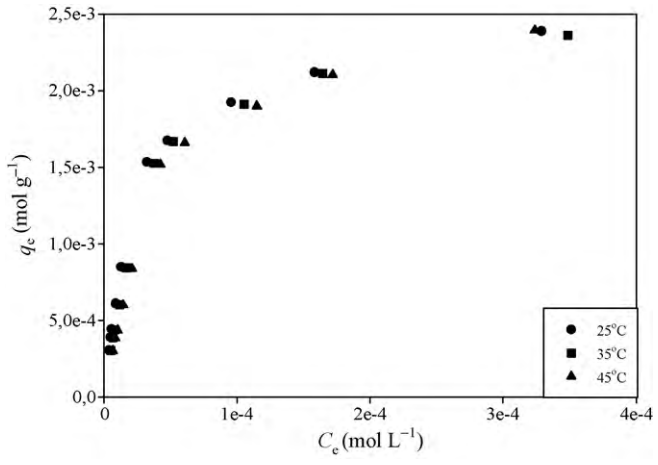

Fig. 6. Adsorption isotherms of the AR88/clay system at different temperatures.

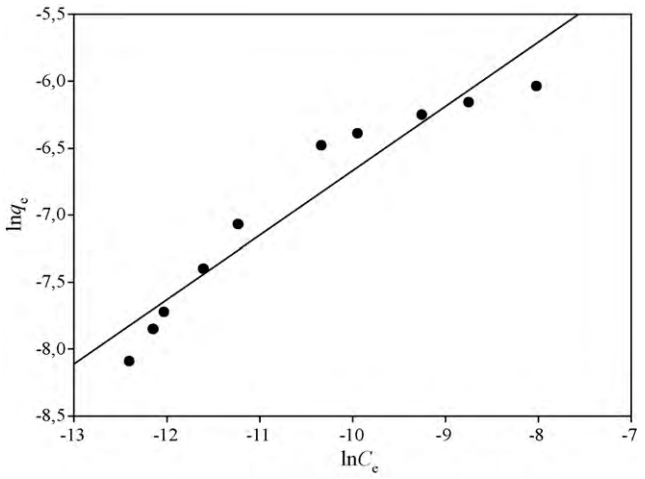

Fig. 7. Freundlich isotherm plot for the adsorption of AR88 onto clay.

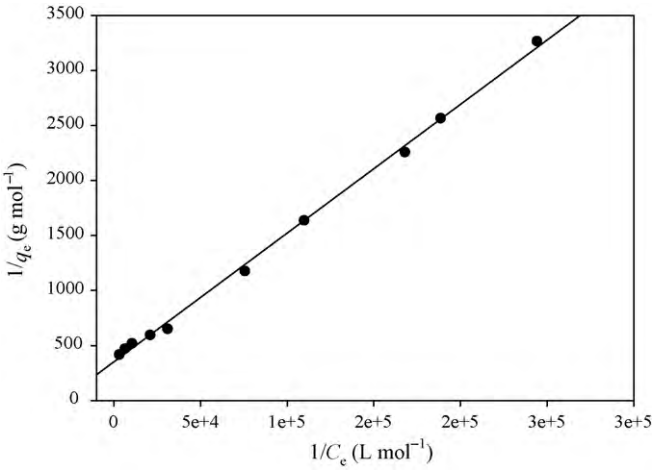

Fig. 8. Langmuir isotherm plot for the adsorption of AR88 onto clay.

Table 3
Sorption capacities for AR88 dye of different materials reported in the literature.

Sorbent material	Sorption capacity (mg g^{-1})	References
Azolla filiculoides	123.50	[1]
Azolla rongpong	78.74	[53]
Azolla microphylla	54.89	[54]
Charfines	33.30	[55]
Lignite coal	30.90	[55]
Bituminous coal	26.10	[55]
Activated carbon	109.00	[55]
Natural clay	1133.10	This study

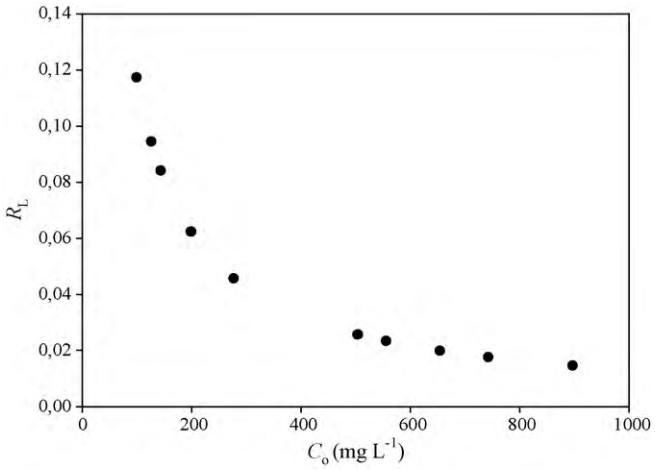

Fig. 9. R_L values at different initial dye concentrations for the adsorption of AR88.

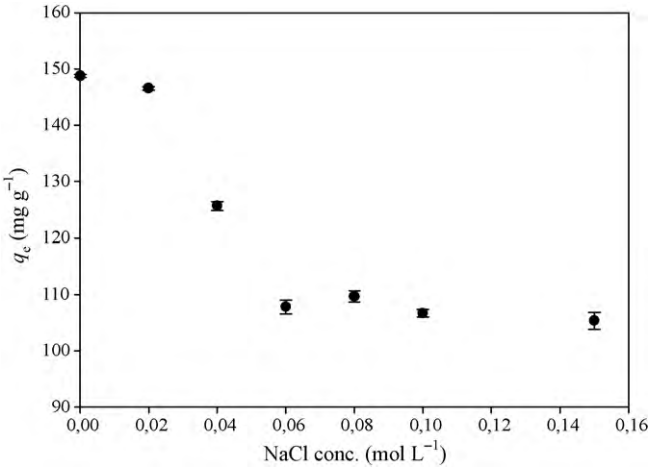

Fig. 11. Effect of ionic strength on the adsorption of AR88 onto clay.

In order to determine the type of adsorption, the equilibrium adsorption data were also tested with the D–R model (Fig. 10). The mean free energy of adsorption (E) is found as 11.41 kJ mol^{-1} at room temperature, which implies that the adsorption of AR88 on clay is chemical ion exchange.

3.7. Effect of ionic strength

Adsorption experiments were performed with the solutions at different ionic strengths since effluents with salt needed to be treated for a good approximation of the experimental data to the real situation. Ionic strength of the dye solutions was altered in a range between 0.02 and 0.15 mol L^{-1} by adding known amount of NaCl solution. The results were shown in Fig. 11. It was seen that the presence of salt in the adsorption medium significantly inhibited the anionic dye adsorption capacity of clay up to 0.06 mol L^{-1} of salt concentration ($p < 0.05$). The adsorption capacity of clay decreased from 148.77 ± 0.49 to 107.82 ± 2.12 mg g^{-1} with an increase in NaCl concentration from 0.00 to 0.06 mol L^{-1}. But even at 0.15 mol L^{-1} of salt, the adsorbent still removed AR88 dye by ~80% yield. Al-Degs et al. reported that if electrostatic forces between the adsorbent and solute ions were attractive, adsorption capacity will decrease with an increase in the ionic strength [49]. The decrease in the dye removal efficiency of adsorbent may also be attributed to the competition between chloride ions and dye anions for the positively charged sites on the adsorbent surface. It was reported that generally, the adsorption mechanism of ion exchange is ionic strength-dependent [50]. The adverse effect of ionic strength on dye removal may be attributed to the ion-exchange mechanism for AR88 adsorption.

3.8. Continuous mode studies

Based on the earlier batch experiments and the respective findings, the column tests were conducted for the removal of AR88. In the first set of the experiments, loading amount of adsorbent into the column was varied from 0.4 to 4.0 g L^{-1}. The findings were presented in Fig. 12. The results indicated that the bed depth strongly influenced AR88 adsorption yield. This was an expected trend since the adsorption performance of adsorbents usually depends on available sorbent amount for adsorption. Column performance for dye removal increased from 70.72 ± 1.28% to 94.24 ± 0.86% with an increase in the adsorbent amount from 0.4 to 1.2 g L^{-1} ($p < 0.05$). The higher adsorption yields for higher bed depth are due to the increase in the surface area of adsorbent providing more available binding sites for the adsorption [51]. After this point the adsorption yield stayed nearly constant ($p > 0.05$) due to the saturation of dye binding sites on the adsorbent surface. Hence, 1.2 g L^{-1} (0.06 g) was selected as the optimum dosage of adsorbent for further column studies.

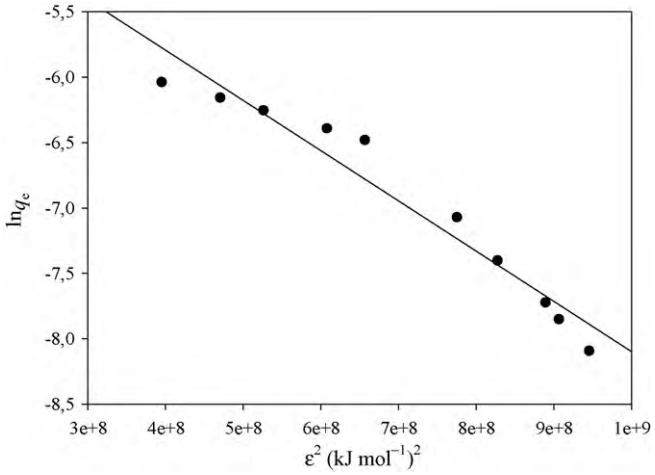

Fig. 10. D–R isotherm plot for the adsorption of AR88 onto clay.

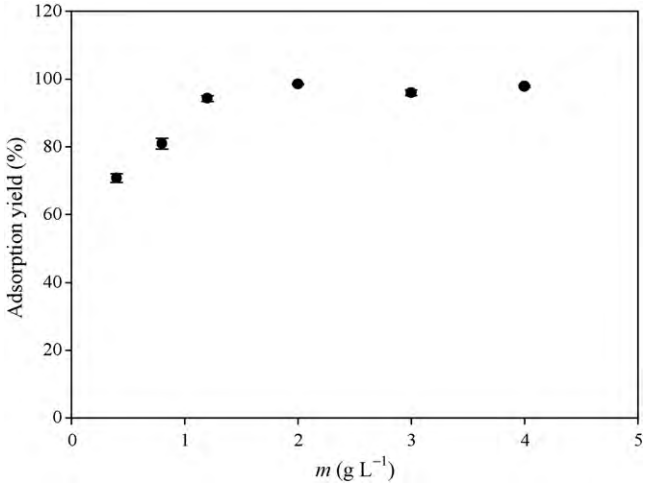

Fig. 12. Effect of adsorbent amount on the adsorption of AR88 onto clay in continuous mode.

The second set of the column experiments was designed to investigate the effect of the flow rate on the dye adsorption potential of clay in continuous mode. The flow rate of sorbate was varied from 0.6 to 8.0 mL min^{-1} while the initial dye concentration (150 mg L^{-1}), adsorbent amount (0.06 g), pH (2.0) were kept constant. The flow rate strongly influenced AR88 uptake capacity, and lower flow rates favor AR88 adsorption. The maximum removal yields were obtained at flow rates of 0.6 and 1.0 mL min^{-1} ($p > 0.05$). The adsorption capacity of clay significantly decreased with increased flow rate ($p < 0.05$). This is due to a decrease in the residence time of dye within the bed at higher flow rates. This causes a weak distribution of the liquid inside the column, which leads to a lower diffusivity of the solute among the particles of the clay [52]. Therefore, AR88 adsorption capacity of clay decreased from 115.34 ± 1.36 to 64.19 ± 0.85 mg g^{-1} with an increase in the flow rate from 1.0 to 8.0 mL min^{-1}. The optimal flow rate for AR88 adsorption was chosen as 1.0 mL min^{-1} in this study.

In order to evaluate the effect of column size on the adsorption performance, column i.d. was varied from 9.0 to 19.0 mm. The AR88 adsorption capacity of clay slightly increased from 115.94 ± 0.62 to 118.53 ± 0.03 mg g^{-1} when the column i.d. was increased from 9.0 to 19.0 mm. But this difference is not found to be statistically significant ($p > 0.05$). This can be an advantage in the selection of suitable column for the application of dye adsorption experiments in continuous flow mode. A small increase in the adsorption capacity of clay with column size can be attributed to an increase in the surface area of the adsorbent filled into the column because the amount of loading adsorbent into column was kept constant.

4. Conclusions

The natural clay used as an adsorbent in this study has an excellent adsorption capacity of 1133.10 mg g^{-1} for AR88 dye. The study also indicated that adsorption process depends upon initial pH, dose of the adsorbent and contact time. pH 2.0 was found to be optimum for the maximum removal of acid dye onto clay. A small amount of natural adsorbent (0.04 g) was enough to attain the decolorization yield of 98.10 ± 0.34 for AR88. Among the kinetic models tested, the adsorption kinetics was best described by the pseudo-second-order equation. The temperature did not significantly affect the adsorption capacity of adsorbent while the rate of adsorption increased with increasing temperature. The Langmuir adsorption isotherm properly described the equilibrium adsorption data and AR88 adsorption was found to be more favorable at higher dye concentrations according to R_L values. Overall, it can be concluded that the clay used in this study showed good performance to remove AR88 from aqueous solution with the advantages of low-cost and large availability.

Appendix A. Kinetic and isotherm model equations

The pseudo-first-order equation:

$$\ln(q_e - q_t) = \ln q_e - k_1 t \quad (2)$$

The pseudo-second-order rate equation:

$$\frac{t}{q_t} = \frac{1}{k_2 q_e^2} + \frac{1}{q_e} t \quad (3)$$

$$h = k_2 q_e^2 \quad (4)$$

The simplified Elovich equation:

$$q_t = \frac{1}{\beta} \ln(\alpha\beta) + \frac{1}{\beta} \ln t \quad (5)$$

The intraparticle diffusion equation;

$$q_t = k_p t^{1/2} + C \quad (6)$$

which k_1 is constant of pseudo-first-order adsorption (min^{-1}), k_2 is the equilibrium rate constant of pseudo-second-order adsorption (g mg^{-1} min^{-1}), q_e and q_t are adsorption capacity at equilibrium and at time t (mg g^{-1}), respectively, h is the initial adsorption rate (mg g^{-1} min^{-1}), α is the initial sorption rate (mg g^{-1} min^{-1}), β is related to the extent of surface coverage and activation energy for chemisorption (g mg^{-1}), C is the intercept (mg g^{-1}) and k_p is the intraparticle diffusion rate constant (mg g^{-1} $min^{-1/2}$).

Freundlich isotherm equation:

$$\ln q_e = \ln K_F + \frac{1}{n} \ln C_e \quad (7)$$

Langmuir isotherm model:

$$\frac{1}{q_e} = \frac{1}{q_{max}} + \left(\frac{1}{q_{max} K_L}\right) \frac{1}{C_e} \quad (8)$$

$$R_L = \frac{1}{1 + K_L C_o} \quad (9)$$

D–R isotherm model:

$$\ln q_e = \ln q_m - \beta\varepsilon^2 \quad (10)$$

$$E = \frac{1}{(2\beta)^{1/2}} \quad (11)$$

where q_e (mol g^{-1}) and C_e (mol L^{-1}) are the amount of adsorbed dye per unit weight of adsorbent and unadsorbed dye concentration in solution at equilibrium, respectively, K_F (L g^{-1}) and n (dimensionless) are Freundlich constants, q_{max} is the maximum monolayer adsorption capacity (mol g^{-1}), K_L is Langmuir constant related to the energy of adsorption (L mol^{-1}), R_L is separation factor, C_o is the initial solute concentration (mol L^{-1}), q_m is the adsorption capacity (mol g^{-1}), β is the activity coefficient related to the adsorption energy (mol^2 kJ^{-2}), E (kJ mol^{-1}) is the mean free energy.

References

[1] T.V.N. Padmesh, K. Vijayaraghavan, G. Sekaran, M. Velan, Batch and column studies on biosorption of acid dyes on fresh water macro alga *Azolla filiculoides*, J. Hazard. Mater. 125 (2005) 121–129.

[2] J. Madhavan, P. Maruthamuthu, S. Murugesan, M. Ashokkumar, Kinetics of degradation of acid red 88 in the presence of Co^{2+}-ion/peroxomonosulphate reagent, Appl. Catal. A 368 (2009) 35–39.

[3] Y.L. Song, J.-T. Li, H. Chen, Degradation of C.I. Acid Red 88 aqueous solution by combination of Fenton's reagent and ultrasound irradiation, J. Chem. Technol. Biotechnol. 84 (2009) 578–583.

[4] M.S. Khehra, H.S. Saini, D.K. Sharma, B.S. Chadha, S.S. Chimni, Biodegradation of azo dye C.I. Acid Red 88 by an anoxic–aerobic sequential bioreactor, Dyes Pigment 70 (2006) 1–7.

[5] A. Pandey, P. Singh, L. Iyengar, Bacterial decolorization and degradation of azo dyes, Int. Biodeter. Biodegr. 59 (2007) 73–84.

[6] O.J. Hao, H. Kim, P.-C. Chiang, Decolorization of wastewater, Crit. Rev. Environ. Sci. Technol. 30 (2000) 449–505.

[7] S.J. Allen, B. Koumanova, Decolourisation of water/wastewater using adsorption, J. Univ. Chem. Technol. Metall. 40 (2005) 175–192.

[8] K.K.H. Choy, G. McKay, J.F. Porter, Sorption of acid dyes from effluents using activated carbon, Resour. Conserv. Recyc. 27 (1999) 57–71.

[9] T. Akar, A.S. Ozcan, S. Tunali, A. Ozcan, Biosorption of a textile dye (Acid Blue 40) by cone biomass of *Thuja orientalis*: estimation of equilibrium, thermodynamic and kinetic parameters, Bioresour. Technol. 99 (2008) 3057–3065.

[10] F. Ferrero, Dye removal by low cost adsorbents: Hazelnut shells in comparison with wood sawdust, J. Hazard Mater. 142 (2007) 144–152.

[11] T. Akar, I. Tosun, Z. Kaynak, E. Kavas, G. Incirkus, S. Tunali Akar, Assessment of the biosorption characteristics of a macro-fungus for the decolorization of Acid Red 44 (AR44) dye, J. Hazard Mater. 171 (2009) 865–871.

[12] B. Chen, C.W. Hui, G. McKay, Film-pore diffusion modeling and contact time optimization for the adsorption of dyestuffs on pith, Chem. Eng. J. 84 (2001) 77–94.

[13] T. Akar, B. Anilan, A. Gorgulu, S. Tunali Akar, Assessment of cationic dye biosorption characteristics of untreated and non-conventional biomass: *Pyracantha coccinea* berries, J. Hazard Mater. 168 (2009) 1302–1309.

[14] S. Tunali Akar, A.S. Özcan, T. Akar, A. Özcan, Z. Kaynak, Biosorption of a reactive textile dye from aqueous solutions utilizing an agro-waste, Desalination 249 (2009) 757–761.
[15] S. Tunali, A.S. Özcan, A. Özcan, T. Gedikbey, Kinetics and equilibrium studies for the adsorption of Acid Red 57 from aqueous solutions onto calcined-alunite, J. Hazard Mater. 135 (2006) 141–148.
[16] A. Adak, M. Bandyopadhyay, A. Pal, Removal of crystal violet dye from wastewater by surfactant-modified alumina, Sep. Purif. Technol. 44 (2005) 139–144.
[17] A. Özcan, A.S. Özcan, Adsorption of Acid Red 57 from aqueous solutions onto surfactant-modified sepiolite, J. Hazard Mater. 125 (2005) 252–259.
[18] Q. Kang, W. Zhou, Q. Li, B. Gao, J. Fan, D. Shen, Adsorption of anionic dyes on poly(epicholorohydrin dimethylamine) modified bentonite in single and mixed dye solutions, Appl. Clay Sci. 45 (2009) 280–287.
[19] S. Tunali Akar, Y. Yetimoglu, T. Gedikbey, Removal of chromium (VI) ions from aqueous solutions by using Turkish montmorillonite clay: effect of activation and modification, Desalination 244 (2009) 97–108.
[20] S.M. Avramescu, N. Mihalache, C. Bradu, M. Neata, I. Udrea, Catalytic ozonation of Acid Red 88 from aqueous solutions, Catal. Lett. 129 (2009) 273–280.
[21] A. Khaldoun, G.H. Wegdam, E. Eiser, M.L. Kerkeb, J.D. Garcia Duran, F. González-Caballero, D. Bonn, Influence of heavy metals adsorption on the surface-energy properties of fluorinated montmorillonite clays "Rassoul", Coll. Surf. A 290 (2006) 1–6.
[22] C.-C. Wang, L.-C. Juang, C.-K. Lee, T.-C. Hsu, J.-F. Lee, H.-P. Chao, Effects of exchanged surfactant cations on the pore structure and adsorption characteristics of montmorillonite, J. Colloid Interface Sci. 280 (2004) 27–35.
[23] J.D.G. Durán, M.M. Ramos-Tejada, F.J. Arroyo, F. González-Caballero, Rheological and electrokinetic properties of sodium montmorillonite suspensions: I. Rheological properties and interparticle energy of interaction, J. Colloid Interface Sci. 229 (2000) 107–117.
[24] A. Jada, H. Debih, M. Khodja, Montmorillonite surface properties modifications by asphaltenes adsorption, J. Pet. Sci. Eng. 52 (2006) 305–316.
[25] A. Kriaa, N. Hamdi, E. Srasra, Acid–base chemistry of montmorillonitic and beidellitic-montmorillonitic smectite, Russ. J. Electrochem. 43 (2007) 167–177.
[26] P. Zarzycki, P. Szabelski, W. Piasecki, Modelling of ζ-potential of the montmorillonite/electrolyte solution interface, Appl. Surf. Sci. 253 (2007) 5791–5796.
[27] F. Thomas, L.J. Michot, D. Vantelon, E. Montargès, B. Prélot, M. Cruchaudet, J.F. Delon, Layer charge and electrophoretic mobility of smectites, Coll. Surf. A 159 (1999) 351–358.
[28] E. Tombácz, M. Szekeres, Surface charge heterogeneity of kaolinite in aqueous suspension in comparison with montmorillonite, Appl. Clay Sci. 34 (2006) 105–124.
[29] G. Crini, Non-conventional low-cost adsorbents for dye removal: a review, Bioresour. Technol. 97 (2006) 1061–1085.
[30] J. Huang, Y. Liu, Q. Jin, X. Wang, J. Yang, Adsorption studies of a water soluble dye, Reactive Red MF-3B, using sonication-surfactant-modified attapulgite clay, J. Hazard Mater. 143 (2007) 541–548.
[31] C.A.P. Almeida, N.A. Debacher, A.J. Downs, L. Cottet, C.A.D. Mello, Removal of methylene blue from colored effluents by adsorption on montmorillonite clay, J. Colloid Interface Sci. 332 (2009) 46–53.
[32] A. Saeed, M. Iqbal, M.W. Akhtar, Removal and recovery of lead(II) from single and multimetal (Cd, Cu, Ni, Zn) solutions by crop milling waste (black gram husk), J. Hazard Mater. 117 (2005) 65–73.
[33] M.H. Khani, A.R. Keshtkar, M. Ghannadi, H. Pahlavanzadeh, Equilibrium, kinetic and thermodynamic study of the biosorption of uranium onto *Cystoseria indica* algae, J. Hazard Mater. 150 (2008) 612–618.
[34] M. Roulia, A.A. Vassiliadis, Sorption characterization of a cationic dye retained by clays and perlite, Micropor. Mesopor. Mater. 116 (2008) 732–740.
[35] S. Lagergren, Zur theorie der sogenannten adsorption gelöster stoffe. Kungliga Svenska Vetenskapsakademiens, Handlingar 24 (1898) 1–39.
[36] Y.-S. Ho, Review of second-order models for adsorption systems, J. Hazard Mater. 136 (2006) 681–689.
[37] S.H. Chien, W.R. Clayton, Application of Elovich equation to the kinetics of phosphate release and sorption in soils, Soil Sci. Soc. Am. J. 44 (1980) 265–268.
[38] W.J. Weber Jr., J.C. Morriss, Kinetics of adsorption on carbon from solution, J. Sanit. Eng. Div. Am. Soc. Civ. Eng. 89 (1963) 31–39.
[39] G.S. ElShafei, I.N. Nasr, A.S.M. Hassan, S.G.M. Mohammad, Kinetics and thermodynamics of adsorption of cadusafos on soils, J. Hazard Mater. 172 (2009) 1608–1616.
[40] N. Kannan, M.M. Sundaram, Kinetics and mechanism of removal of methylene blue by adsorption on various carbons—a comparative study, Dyes Pigment 51 (2001) 25–40.
[41] S.V. Mohan, N.C. Rao, J. Karthikeyan, Adsorptive removal of direct azo dye from aqueous phase onto coal based sorbents: a kinetic and mechanistic study, J. Hazard Mater. 90 (2002) 189–204.
[42] C.H. Giles, D. Smith, A. Huitson, A general treatment and classification of the solute adsorption isotherm. I. Theoretical, J. Colloid Interface Sci. 47 (1974) 755–765.
[43] C. Hinz, Description of sorption data with isotherm equations, Geoderma 99 (2001) 225–243.
[44] G. Limousin, J.-P. Gaudet, L. Charlet, S. Szenknect, V. Barthès, M. Krimissa, Sorption isotherms: a review on physical bases, modeling and measurement, Appl. Geochem. 22 (2007) 249–275.
[45] H.M.F. Freundlich, Über die adsorption in Lösungen, Z. Phys. Chem. 57 (1906) 385–470.
[46] I. Langmuir, The adsorption of gases on plane surfaces of glass, mica and platinum, J. Am. Chem. Soc. 40 (1918) 1361–1403.
[47] M.M. Dubinin, L.V. Radushkevich, Equation of the characteristic curve of activated charcoal, Proc. Acad. Sci. Phys. Chem. Sec. U.S.S.R. 55 (1947) 331–333.
[48] K.R. Hall, L.C. Eagleton, A. Acrivos, T. Vermeulen, Pore- and solid-diffusion kinetics in fixed–bed adsorption under constant-pattern conditions, Ind. Eng. Chem. Fundam. 5 (1966) 212–223.
[49] Y.S. Al-Degs, M.I. El-Barghouthi, A.H. El-Sheikh, G.M. Walker, Effect of solution pH, ionic strength, and temperature on adsorption behavior of reactive dyes on activated carbon, Dyes Pigment 77 (2008) 16–23.
[50] E. Pehlivan, B.H. Yanık, G. Ahmetli, M. Pehlivan, Equilibrium isotherm studies for the uptake of cadmium and lead ions onto sugar beet pulp, Bioresour. Technol. 99 (2008) 3520–3527.
[51] Z. Zulfadhly, M.D. Mashitah, S. Bhatia, Heavy metals removal in fixed-bed column by the macro fungus *Pycnoporus sanguineus*, Environ. Pollut. 112 (2001) 463–470.
[52] A.M. El-Kamash, Evaluation of zeolite A for the sorptive removal of Cs^+ and Sr^{2+} ions from aqueous solutions using batch and fixed bed column operations, J. Hazard Mater. 151 (2008) 432–445.
[53] T.V.N. Padmesh, K. Vijayaraghavan, G. Sekaran, M. Velan, Application of *Azolla rongpong* on biosorption of acid red 88, acid green 3, acid orange 7 and acid blue 15 from synthetic solutions, Chem. Eng. J. 122 (2006) 55–63.
[54] T.V.N. Padmesh, K. Vijayaraghavan, G. Sekaran, M. Velan, Application of two- and three-parameter isotherm models: biosorption of Acid Red 88 onto *Azolla microphylla*, Biorem. J. 10 (2006) 37–44.
[55] S.V. Mohan, P. Sailaja, M. Srimurali, J. Karthikeyan, Color removal of monoazo acid dye from aqueous solution by adsorption and chemical coagulation, Environ. Eng. Policy 1 (1999) 149–154.